Designing of Power System Stabilizer based on the Root Locus Method with Lead-Lag Controller and Comparing it with PI Controller in Multi-Machine Power System

Shadi Jalali[b,*], Ghazanfar Shahgholian[b]

[a]Smart Microgrid Research Center, Najafabad Branch, Islamic Azad University, Najafabad 85141-43131, Iran
[b]Department of Electrical Engineering, Najafabad Branch, Islamic Azad University, Najafabad 85141-43131, Iran

Abstract

This paper presents a method for designing a multi-machine power system stabilizer. The conventional design technique using a single machine infinite bus approximation involves a frequency response estimation called GEP(s). Frequency response is estimated between the input AVR and electrical output torque. The power system stabilizer is designed by frequency response and based on the root locus method to improve the damping of oscillatory modes. By using this method, we can adjust the structure of the PSS compensator and its parameters in the multi-machine system and it does not need to know the equivalent reactance of output and voltage of the infinite bus or the other estimations in every machine. In the proposed method, information available at the high voltage bus of the step-up transformer is used to set up a modified Heffron-Phillips model. Finally, this method is examined on three test systems. Simulation results indicate the performance and effectiveness of the proposed method.

Keywords: Four-leg Shunt Active Power Filter (4LSAPF); Enhanced Phase Locked Loop (EPLL); Self Tuning Filter (STF); Fuzzy Logic Control (FLC); Harmonics; Reactive power.

1. Introduction

When several generators are connected together, their interactions can cause disturbances in the performance of control systems. Therefore, proportional adjustment between generators in control systems is very useful [1, 2]. A generator swinging against the rest of the system causes local mode oscillations and, in interarea mode oscillations, groups of generators swinging against each other. These oscillations exist continuously in the system, but if the variation of load and generation rate causes the location of oscillating systems modes to change, moving them toward the right of the imaginary axis, then the system will be unstable [3, 4]. Therefore, it is necessary to increase the amount of damping of the oscillating modes [5, 6].

So, a control system called a power system stabilizer is used that add extra damping to the excitation system. Power system stabilizers are built to help damp these oscillations on the excitation system [7, 8]. This equipment provides additional damping to the system through lead compensation, which is caused between the input speed and output
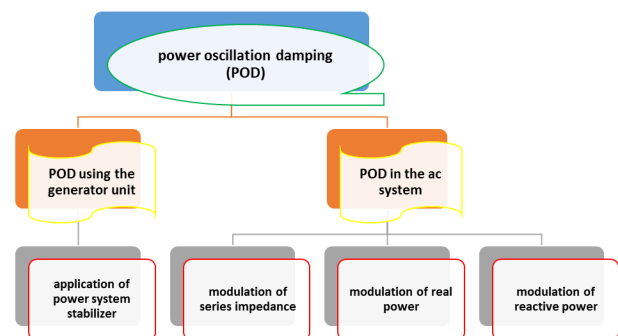

Figure 1: Power oscillation damping strategies

torque. Several methods have been used to design stabilizers [9, 10].

With the advent of power electronics and the production of equipment with high current and voltage, the usage of flexible alternating current transmission (FACTS) has become economically justified. Conventional PSS could not provide appropriate damping for interarea oscillations, so a combination of PSS and FACTS is used to provide optimal damping. In other words, the use of PSSs alone may not be effective in some cases in providing sufficient damping for power oscillations, specifically for long distance power transmis-

sion [11, 12]. The concept of FACTS became feasible due to the application of high-power electronic devices for power flow, voltage control, and additionally enhancing the damping of power oscillations [13]. In the literature several researchers propose the coordination of PSS with FATCS controllers to enhance the dynamic performance of the power system. In [14], the authors discussed a global tuning procedure for PSS and FACTS devices using a parameter-constrained nonlinear optimization algorithm. A robust coordinated design of a PSS and TCSC based stabilizer is thoroughly investigated in [15]. Generally, there are two kinds of power oscillation damping controllers in power systems, as shown in Fig. 1: PSS and FACTS controllers.

The main goal of most studies in recent years is the adjustment of a secondary control system for the excitation system in order to stabilize the oscillating modes. PSS is not usually installed in all generators, but is only installed in the generators that can cause the maximum amount of damping in the system and the oscillatory modes [16, 17]. The structure of PSS commonly includes a washout filter and a lead-lag block diagram. The PSS input signals can include terminal voltage, rotor speed deviation and electrical power [18, 19]. In previous studies a linear combination of these signals is used as an input signal. The stabilizer is adjusted for lag compensation which is created between the generator, excitation system and power system [20]. Typical stabilizers are divided into two categories: analog and digital. In this study, we discuss only analog PSS. Analog PSS parameters are adjusted by using linear and nonlinear methods. In previous studies several methods were proposed based on linear methods in order to design PSS, including pole placement, pole shifting, optimal linear control, eigenvalues sensitivity analysis and characteristic method. In recent studies, the proposed methods are typically used for single-machine infinite-bus power systems.

This paper presents an approach to adjust the parameters of multi-machine power system stabilizers based on the root locus method and frequency response of the system. Adjustment of PSS parameters requires accuracy and good knowledge of the structure and dynamic model of the system. Therefore, accurate modeling of the power system has to be done before the desired design of PSS can be achieved.

2. Proposed Method

The flowchart of the proposed method is shown in Fig. 2. The transfer function which will be described below is obtained for all the system generators in which PSS will be installed. Finally, the parameters of the power system stabilizer are adjusted by using the root locus method and frequency response of the system. The PSS parameters are obtained for an operation point and operating conditions of the system. Therefore, several different scenarios of loading in the system are considered and parameters are adjusted for the worst loading conditions so that the system can respond to
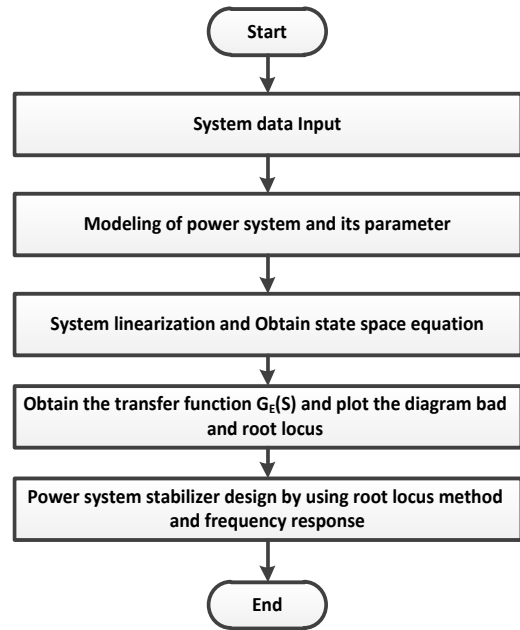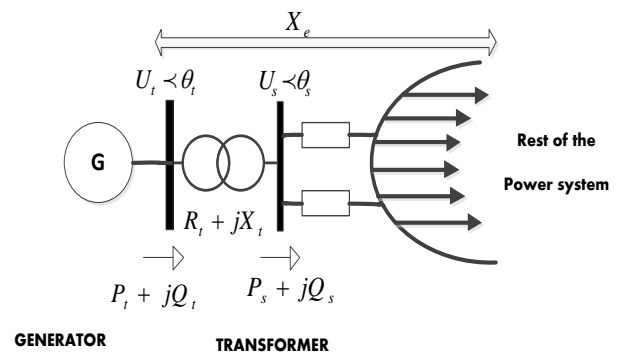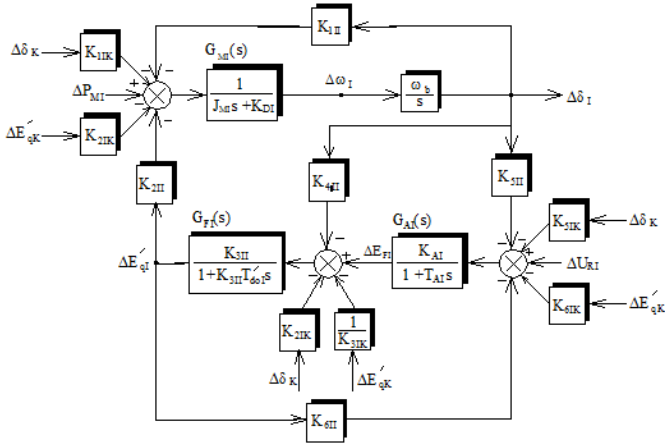

Figure 2: The flowchart of the proposed method

Figure 3: Single machine in a connected network

disturbances in the various operating conditions of the system.

3. Power System Model

Small-signal stability analysis requires dynamic modeling of the major components of the power system. These main components are: synchronous generator, excitation system, automatic voltage regulators and other components [21]. The model shown in Fig. 3 is used to obtain the linearized Heffron-Phillips or K-constant model.

In order to analyze small signal stability, it is necessary to consider the effect of the excitation system, which indirectly controls the reactive power output of the generator [22]. The linearized dynamic equations of single machine infinite bus (SMIB) are as follows [23, 24]:

Figure 4: Linearized model of *i*th synchronous machine

Figure 5: The PSS Structure

Figure 6: Electrical transfer function in single-machine infinite-bus power system

$$\frac{d}{dt}\delta = 2\pi f_o \delta \tag{1}$$

$$\frac{d}{dt}\omega = \frac{1}{2H}(P_M - P_E - K_D\omega) \tag{2}$$

$$\frac{d}{dt}E_F = \frac{1}{T_E}[-E_F + K_E(U_R - U_T)] \tag{3}$$

$$\frac{d}{dt}E'_q = \frac{1}{T'_{do}}[E_F - E'_q + (X'_d - X_d)i_d] \tag{4}$$

In Fig. 4, the constants of the linearized model depend on the machine parameters and operating conditions of the system [25, 26].

4. Power System Stabilizer (PSS) design

Due to the continual variation of dynamic system conditions, the operation point of the system and the load and generation levels change constantly, causing low-frequency oscillations in the system. Hence, PSS is designed and adjusted to add suitable damping to the system so that low-frequency oscillations do not cause small-signal instability. PSS is an additional control block that is added to improve system stability [27].

4.1. Design based on the general structure of the Power System Stabilizer

The main structure of the power system stabilizer is shown in Fig. 5. The transfer function $G_E(s)$, shown in Fig. 6, was affected by assuming that variation of machine speed is zero. It is given by Shahgholian et al. [28]:

$$G_E(s) = \frac{K_2 K_3 E(s)}{(1 + sT'_{d0}K_3) + K_3 K_6 E(s)} \tag{5}$$

where $E(s)$ is the transfer function of the excitation system. According to (5), for every machine in the multi-machine system, $G_E(s)$ can be calculated based on the power flow data
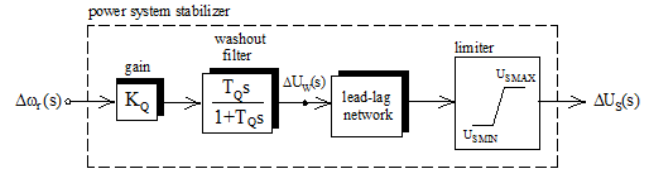
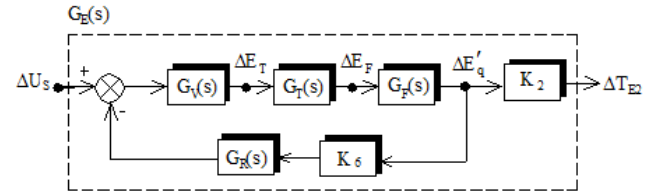in the transformer bus and initial condition of the generator. The compensator structure that is required for the resonant or non-resonant form of $G_E(s)$ is given in (6) and (7).

$$H(s) = K_{pss}\frac{sT_\omega}{1 + sT_\omega}\frac{(\frac{1}{\omega_n^2}s^2 + \frac{2\zeta}{\omega_n}s + 1)}{(1 + sT_1)(1 + sT_2)} \tag{6}$$

$$H(s) = K_{pss}\frac{sT_\omega}{1 + sT_\omega}(\frac{1 + sT_1}{1 + sT_2})^m \tag{7}$$

In (7), m is the number of lead-lag stages. After plotting the frequency response of the transfer function $G_E(s)$ for every generator, if it is without resonance peak, we can use the procedure of Fig. 7.

4.1.1. Selection of stabilizer time constants

At first f_c and β are adjusted so that compensated phase of $G_E(s)$ at the frequency of the local mode (7 rad/sec) is less than 50 degrees and intersection at 90 degrees occurs above 22 rad/sec (3.5 Hz). Phase margin of higher than 30° is suitable for compensated $G_E(s)$. Here f_c is the central frequency of the compensator. The equations to obtain constants T_1 and T_2 are given in [29].

4.1.2. Plotting the root locus

Plot the root locus of the plant with compensator from A and matrices with slip speed as output. Now look for the departure of root locus branch at the modes near the imaginary axis. If it is not in the increasing damping direction adjust the zero of the compensator.

4.1.3. Gain Selection of compensator

The gain from the root locus plot is selected so that the damping ratio of rotor mode is maximized.
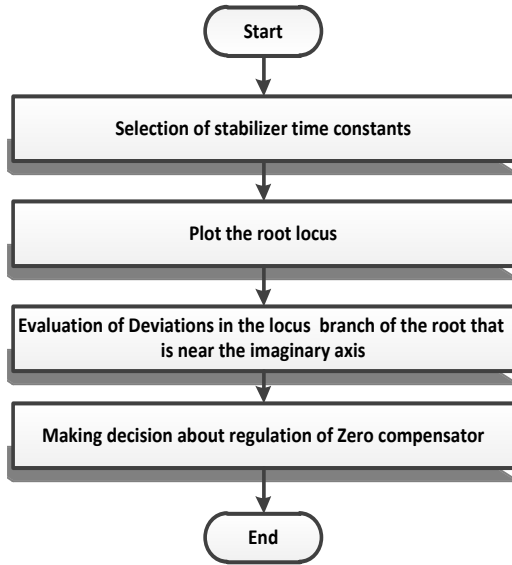
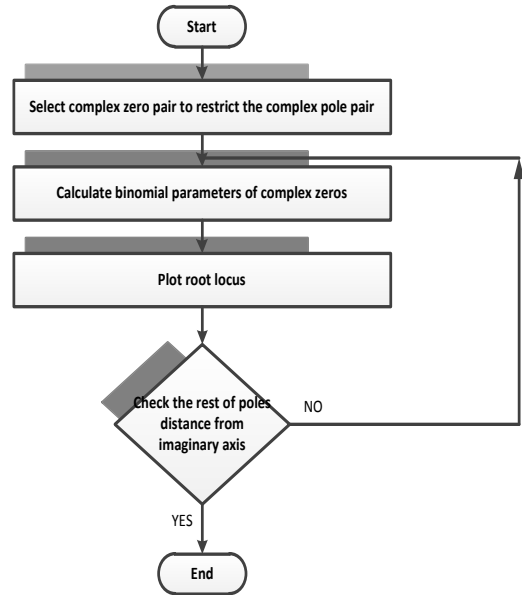Figure 7: Design procedure of stabilizer for $G_E(s)$ without resonant

Figure 8: Procedure of stabilizer design for $G_E(s)$ with resonance

4.2. Power system stabilizer design for $G_E(s)$ with resonance peak

This condition occurs when the matrix has two pairs of complex eigenvalues with significant damping. In this case the proposed procedure in Fig. 8 is used to adjust the parameters of the power system stabilizer.

4.2.1. Restricting the complex pair of poles by zeros of compensator

The first step is to decide the complex pair of poles to be constrained by zeros. In order to determine the dominant pole of the system, a set of matrices is created as the transformer reactance is increased. The eigenvalues of this matrix are plotted. A pair of eigenvalues that are oriented toward the positive axis should be chosen as a pair that must be restricted by a zero pair.

4.2.2. Finding values of ξ and ω_n

This step is to find values of ξ and ω_n of the second order transfer function; these values are significantly in accordance with the phase characteristic of $G_E(s)$. Now fix one of the poles say T_1 at 0.01 and adjust T_2 and ω_n of the numerator so that the compensated GEP has good phase margin (about 40 degrees).

4.2.3. Plotting the root locus and evaluation of branch deviation of root locus

After plotting the locus, the locus branch is checked to ensure it passes across the required complex pole. Otherwise, T_2 and ω_n are adjusted based on that. Moreover, the locus branch of the other complex poles must be far enough from the location of the complex zeros.

4.3. Using the PI controller for power system stabilizer design

In this study, the PI controller is used instead of the lead-lag controller in the power system stabilizer block. PI controller transfer function is indicated by $G_E(s)$ and is as per (9):

$$G_c(s) = K_p + K_i \frac{1}{s} = \frac{K_p s + K_i}{s} \qquad (8)$$

By rewriting (8), the PI controller transfer function can be obtained as (9):

$$G_c(s) = K_p \frac{s + \frac{K_i}{K_p}}{s}, \qquad K_i \leq K_p \qquad (9)$$

Where K_P is the static gain and K_i/K_p indicate a stable zero that is close to the origin.

$$G_c(s) = \frac{s + z_c}{s} \qquad (10)$$

The algorithm for designing this controller is given in the following section.

- Pole of PI controller is set at zero value and the value of zero is considered arbitrarily in a small amount close to the origin, for example Z_c=0.01 or Z_c=0.1.

- If necessary, the static loop gain K_P is set at a value except one so that the desired value of steady error compensation is achieved.

Generally, PI controller design is an experimental procedure that is based on trial and error in order to achieve the desired phase margin.
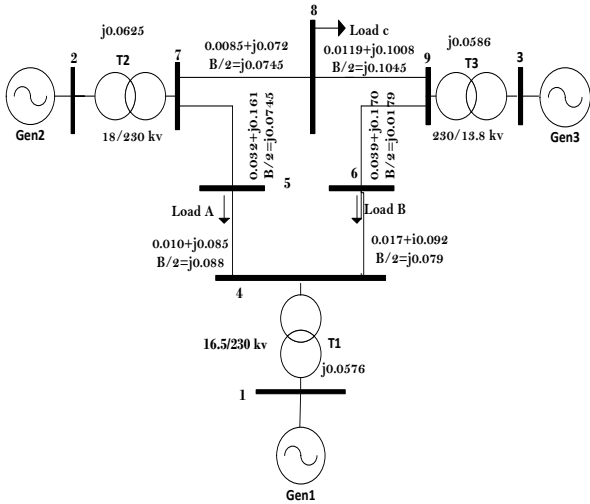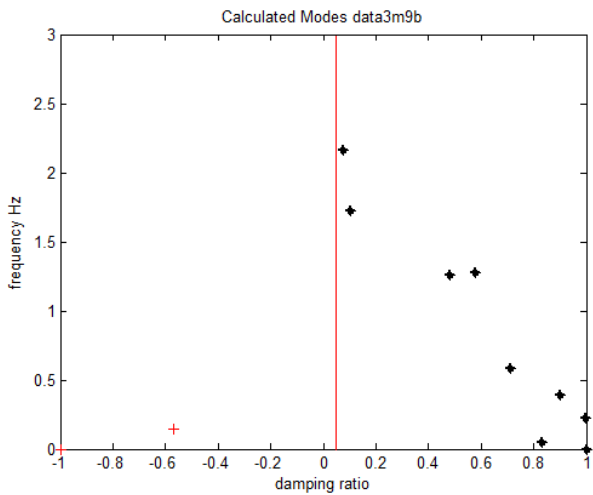
Figure 9: Three-Generator Nine-Bus System

Figure 10: Modal analysis

5. Case Studies and Simulation Results

The proposed method was implemented in three systems: 3, 5, 10 machines and the results analyzed. First, small-signal stability analysis is done without PSS. Then, PSS is adjusted and small-signal stability is checked again to observe the adjustment effect. Finally, several different loading scenarios are evaluated in order to evaluate the effectiveness of PSS adjustment. Finally the results of the lead-lag controller are compared with the results of the PI controller

5.1. Three-Generator Nine-Bus Power System

This system is the first case study that is used to evaluate power system oscillations and the implementation of the proposed method for stabilizer design. This system is taken from [30]. This is the most widely used test system for validating several control designs (Fig. 9). In this study the exciter is considered as a first order block diagram, with a gain and time constant of 200 and 0.05. Frequency response
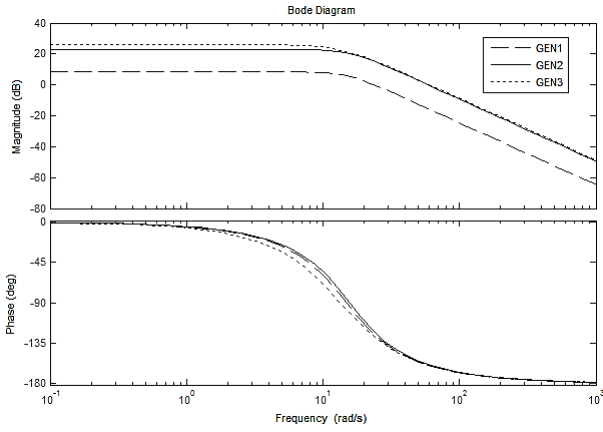
Table 1: Eigenvalues, frequency, and damping ratio

Damping	Frequency (Hz)	Eigenvalues
-1	0	0.0058
	Instable	
0.0359	1.366	-0.308+j8.857
	Marginally stable	
0.0359	1.366	-0.308-j8.857
	Marginally stable	

Table 2: Eigenvalues of Three-generator system for each generator

	Eigenvalue
G_1	0.0500±j7.4200 , -10.0100±j11.8900
G_2	-1.3430±j11.0500 , -9.4191±j4.4815
G_3	-1.7000±j14.8000 , -15.1, -4.3

estimation and calculating the coefficients of the Heffron-Phillips model require data obtained with power flow. PST Toolbox of MATLAB is used for small signal stability analysis. Modal analysis is used to evaluate small-signal stability without PSS. Damping factors of eigenvalues are shown in Fig. 10. In this paper the minimum damping factor criterion is considered 0.05. As can be seen from Fig. 3, there is an unstable eigenvalue which indicates the instability of the system. In addition, two pairs of eigenvalues are less than 0.1; these eigenvalues are known as the critical eigenvalues. Table 5.1 shows these eigenvalues, the frequency, and their damping factors.

Eigenvalues, un-damped frequencies and the damping ratio of each generator are shown in Tables 5.1 and 5.1 by considering the high voltage bus of the step-up transformer as a slack bus and linearization state equations.

The results of the small-signal stability analysis are used to determine that this system has unstable eigenvalues. The frequency responses of generators are given in (11) to (13) and Fig. 11.

$$G_E(s) = \frac{152}{17.67 + 3.26s + 0.04905s^2} \quad (11)$$

$$G_E(s) = \frac{193.43}{0.057s^2 + 1.1912s + 14.047} \quad (12)$$

$$G_E(s) = \frac{221}{0.06s^2 + 1.2362s + 10.83} \quad (13)$$

None of the frequency responses of the generators of three machines have resonance peak. In this case, generator 3 has the most steady-state stability due to its greatest gain. But from the point of time constant, all generators have poles that are close together in approximate terms; so the delays of the three generators are in approximately the same interval.

For the first generator, the phase margin is 22 degrees and the gain margin is infinite; so 30 degrees should be added by

Table 3: Un-damped frequencies and damping ratio

	ζ_0	ω_n
G1	-0.00673	7.43
G2	0.1207	11.1310
G3	0.1141	14.8963

Figure 11: $G_E(s)$ of three-generator nine-bus system
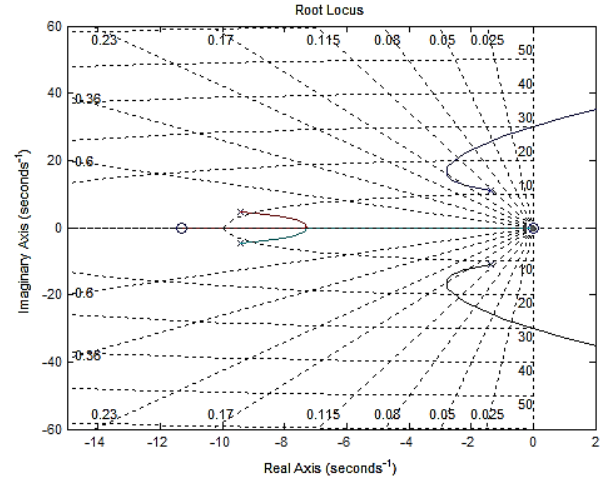

Figure 12: Root locus GEN-1, three-generator nine-bus system
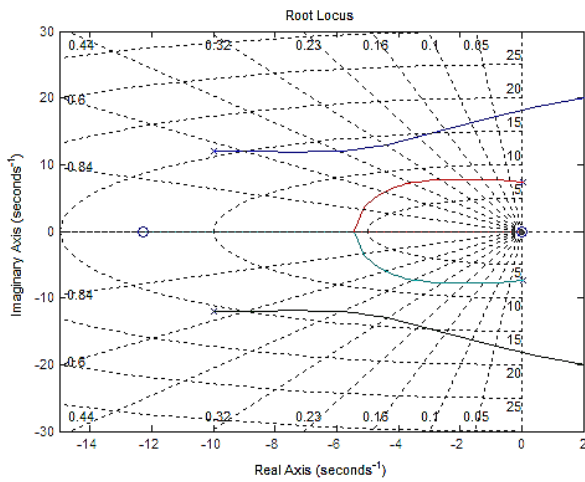

Figure 13: Root locus GEN-2, three-generator nine-bus system
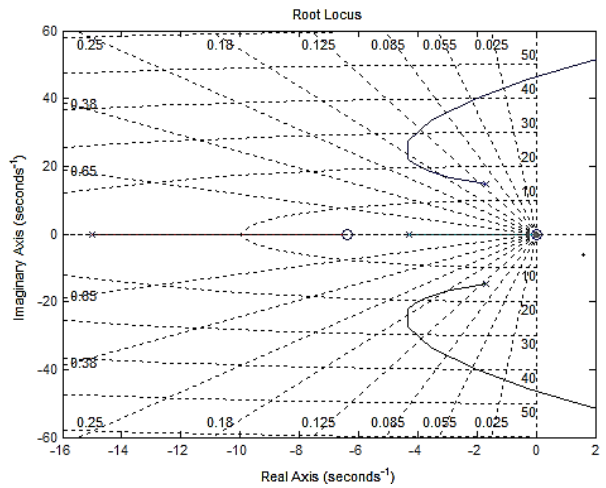

Figure 14: Root locus GEN-3, three-generator nine-bus system

the stabilizer. Therefore, β is considered 30 degrees. Based on the proposed method, central frequency is also considered to be 3.5 Hz. In the next stage, the gain of PSS should be calculated. In this study, the PSS gain is obtained from the root-locus diagram and regards the desired amount of the damping ratio (ξ=0.15). Finally, by addition of the pole and zero of the stabilizer, the root-locus of generators 1, 2 and 3 are shown in Figs 12, 13, and 14. According to the results of the root locus, it can be observed that PSS increases system damping, so that the refraction angle of roots which are close to the imaginary axis is 180 degrees. Fig. 15 shows the frequency response of generator 1 after applying the stabilizer.

After applying the stabilizer, the suitable condition of the problem is satisfied, i.e., the phase margin is about 40 degrees and the refraction angle occurred at 22 rad/sec with a slope close to 180 degrees. Therefore, the designed compensator will provide suitable damping in the system.

The effectiveness of the proposed PSS design is shown in Figs. 16 and 17 with small disturbances, such as a 10% step change in V_{ref} in GEN3.

To evaluate the performance of the designed compen-

sator, a three-phase short circuit is considered for the three machines system. This fault happened at the first second in bus 7 and after 100 ms it will be cleared. Figs. 18 and 19 show the impact of a three-phase short circuit fault before and after applying a stabilizer on the voltage of buses 7 and 8. The electrical power response of generator 3 for a 3ϕ self-cleared is shown in Fig. 20. Fig. 21 shows transferred power between bus 7 and bus 8 respectively after the three-phase fault and after applying the stabilizer. The PSS data are shown in Table 5.1 for the three machines system.

Table 4: PSS parameters 3 GEN 9 bus system

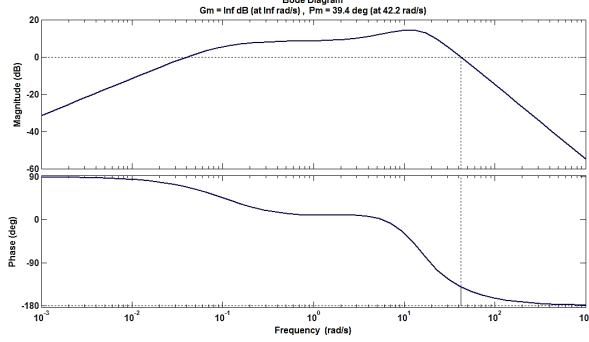| G	β	T_1	T_2	K_{PSS}
1	30	0.0803	0.0257	49
2	35	0.08735	0.0236	5
3	37	0.15	0.01	3

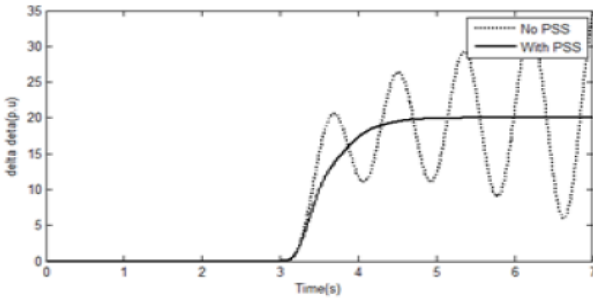Figure 15: Frequency response of generator 1 after applying the stabilizer

Figure 16: Response variations of GEN-1 rotor angle to 10% step change in Vref at GEN-3

5.2. Five-Generator Ten-bus System

This system is shown in Fig. 22 [31]. Due to the critical eigenvalues of Table 5.2, it is observed that the system has 4 oscillating modes where its damping ratio is less than 2.0. Figs 23 and 24 indicate frequency responses of generators 1, 2, 3, 4 and 5. Generators 2, 3 and 5 have the resonance peak in their frequency responses.

In order to adjust the parameters of the stabilizer, the reactance of the transformer should be changed step by step and complex eigenvalues of the matrix should be evaluated. Figs. 25, 26, and 27 show the reactance changes of generators 2, 3 and 5.

Fig. 25 shows that as x_t is increased, pole -1.250±j9.430 move in negative direction of real axis, and pole -1.935±j5.760 move in positive direction of real axis. Consequently, pole −1.935±j5.760 is the dominant pole and this pole should
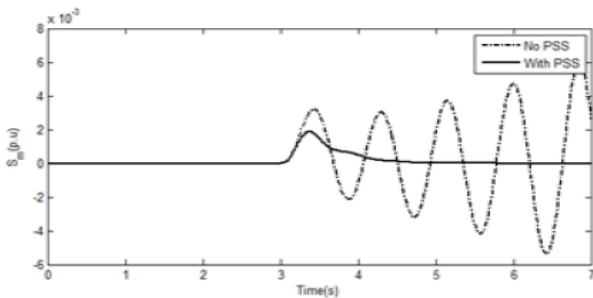

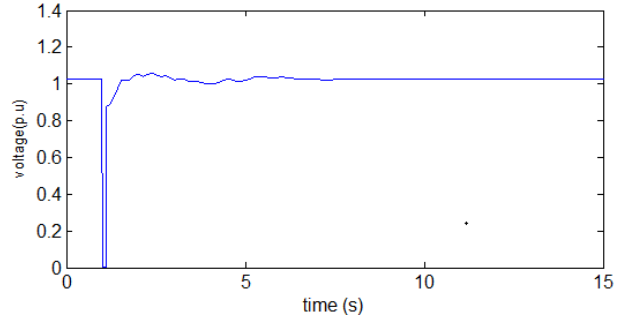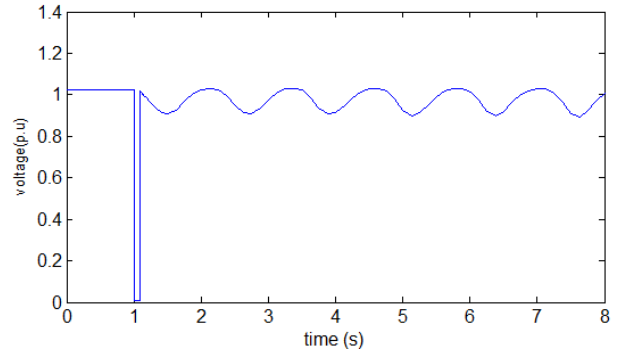Figure 17: Speed slip variations of GEN-1 due to 10% step change in V_{ref} at GEN-3

Figure 18: Voltage of bus 7 for a 3ϕ self-cleared fault at bus 7; (a) without PSS; (b) with PSS

Table 5: Eigenvalues, frequency, and damping ratio

eigenvalues	Damping	Stability Type
-0.30+j3.5	0.084	Marginally Stable
-0.06+j5.33	0.012	Marginally Stable
-0.38+j7.2	0.052	Marginally Stable
-0.8+j10.66	0.171	Marginally Stable

be restricted by complex zero of the compensator. Fig. 26 shows that -0.850±j10.750 is the dominant pole and this pole should be restricted by complex zero of the compensator. Fig. 27 shows that -2.256±4.835 is the dominant pole and this pole should be restricted by complex zero of the compensator. Here, a stabilizer is designed for generator 5 and the complete procedure of design is studied. The algorithms and design procedures of the other generators are the same as for generator 5. In the first step it should be determined how much of required phases margin is provided by transfer function $G_E(s)$, then the rest of the required phase margin should be compensated by the stabilizer. For this purpose, the frequency response of generator 5 is plotted and the gain margin is calculated. In Fig. 28 it can be observed that the phase margin of this generator is about 9 degrees. For this purpose, the parameters T_1, T_2, ω_n and ξ should be adjusted so that the required 40 degrees will be compensated. Hence, as can be seen in Figs. 29 and 30, five different states are

Table 6: Specifications of stabilizer parameters for the design process

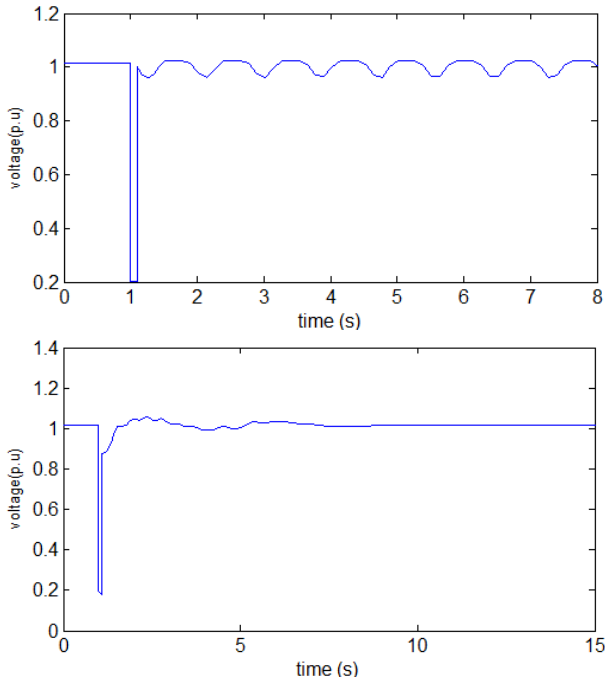|	T_1	T_2	ω_n	ξ	Phase margin
Case 1	0/01	0.01	7.7	0.4	9.35
Case 2	0.01	0.05	11	0.4	13.4
Case 3	0.01	0.08	15	0.5	21.9
Case 4	0.01	0.1	18	0.6	24.2
Case 5	0.01	0.17	22	0.4	39.4

Figure 19: Voltage of bus 8 for a 3ϕ self-cleared fault at bus 7; (a) without PSS; (b) with PSS.
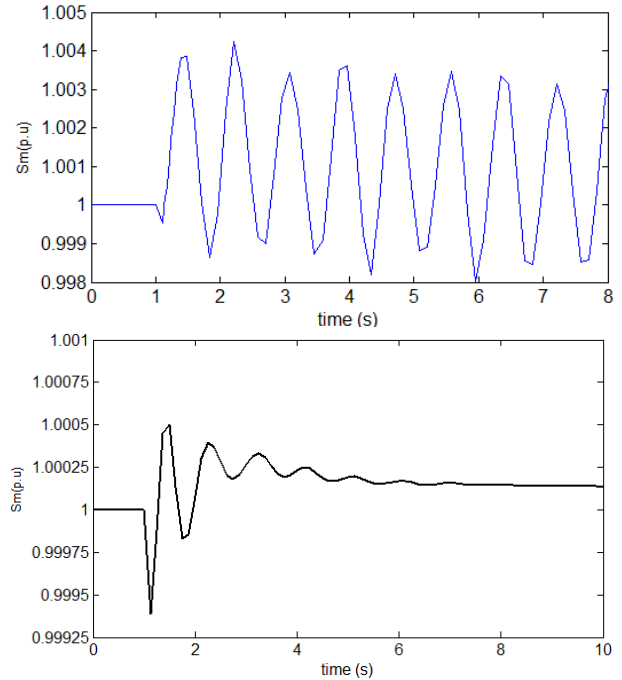

Figure 20: Electrical power response of generator 3 for a 3ϕ self-cleared; (a) without PSS; (b) with PSS

Table 7: PSS parameters of the 5 machines system stabilizers

Num. G	T_1	T_2
1	0.01	0.17
2	0.01	0.05
3	0.11	0.08
4	0.12	0.09
5	0.09	0.06

evaluated. Finally, in the fifth state, the system phase margin reaches 40 degrees. Data on the adjustment and phase margin of each state are given in Table 5.2.

The PSS data are shown in Table 5.2 for the five machines system.

Fig. 31 shows the roots locus of GEN-5 in the fifth state. It is observed that the zeros are close to the complex poles and compensated.

5.3. Ten-Generator 39 Bus System

This system is taken from Padiyar [32]. In this system, PSS is modeled for all generators except generator number 2 that is modeled as the external network model (infinite bus). In this system frequency responses of generators have no

Table 8: Characteristics of stabilizer parameters for the 10 machines system

G'	T_W	T_1	T_2	K_{PSS}
1	10	0.166	0.0677	66.4
3	10	0.163	0.0687	49
4	10	0.163	0.0688	60
5	10	0.163	0.0688	38.8
6	10	0.167	0.0672	70
7	10	0.158	0.0713	50.9
8	10	0.166	0.0678	41.9
9	10	0.165	0.0679	38.4
10	10	0.128	0.0876	29.1

resonance peak. The characteristics of the designed stabilizer parameters are given in Table 5.2. To evaluate the effectiveness of the obtained adjustment, different loading conditions are examined in the system. Three scenarios of low load, medium load and heavy load are considered for the system load level.

In Fig. 32 slip speed of GEN-8 is considered at normal and heavy load condition without PSS, by a 10% change in mechanical torque. It is shown that slip speed of GEN-8 at the normal condition starts to oscillate, but after a while it will be damped. Now, slip speed response of GEN-8 to 10% step in T_m is considered at heavy loading conditions with PSS.

Fig. 33 shows slip speed of this generator's response to a 10% step change in mechanical torque, at heavy condition with and without the proposed PSS.

It can be seen that slip speed variations caused by a 10% step change in mechanical torque are damped after a while with the proposed PSS.

Under light loading condition, slip speed variation of GEN-6 for a 10% step change in ΔT_m that occurred at second 5, before and after applying the stabilizer is shown in Fig. 34.

The performance of the proposed PSS is shown in Fig. 34. The slip speed variations of GEN-6 with PSS designed based on the proposed method damps in a shorter time compared to the situation without PSS.

6. Stabilizer design based on PI Controller for Three-Machines Power System

PI controller is designed for the three generators of the three machines system, and the results of the PI controller
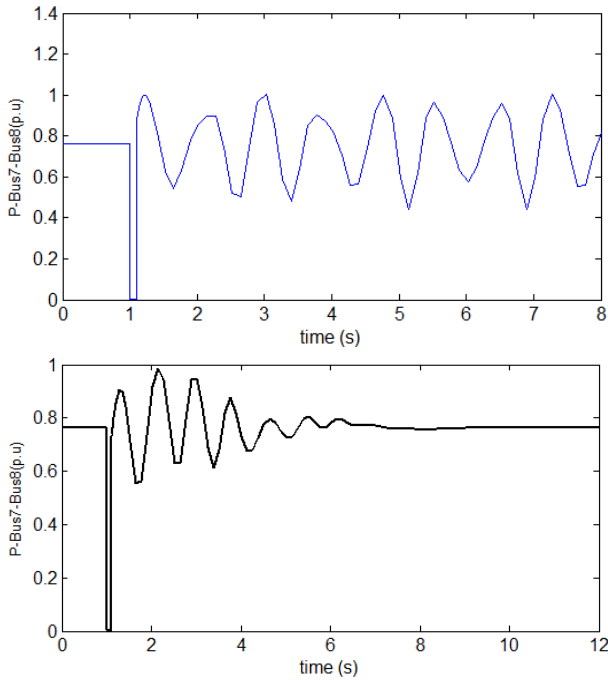
Figure 21: Transferred power between bus 7 and bus 8; (a) without PSS; (b) with PSS
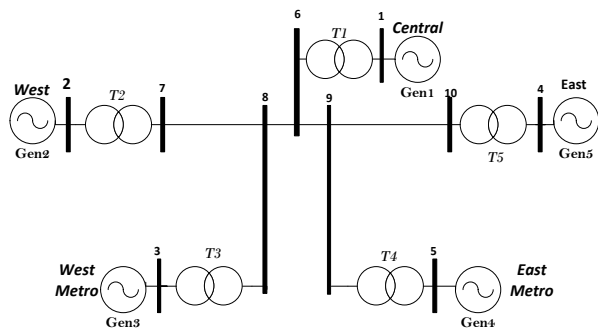

Figure 22: Five-Generator Ten-bus system

parameters are given in Table 6 for the three machines system. A three phase fault is implemented on bus 3. Fig. 35 shows slip speed responses of GEN-1 to GEN-3 for a 3ϕ fault in the presence of the designed stabilizer based on the general structure of the PSS. Fig. 36 shows the slip speed responses of GEN-1 to GEN-3 for a 3ϕ fault in the presence of the PI controller.

By comparing Figs. 34 and 35, it can be observed that the PI controller partially improves system damping conditions, but it cannot completely eliminate the low frequency oscillations. In fact, this type of controller has a major impact on the steady-state behavior of the system and it improves steady-state error. Thus, if the low-frequency oscillation is low and oscillatory modes are local, using the PI controller can have a desirable effect on system stability.
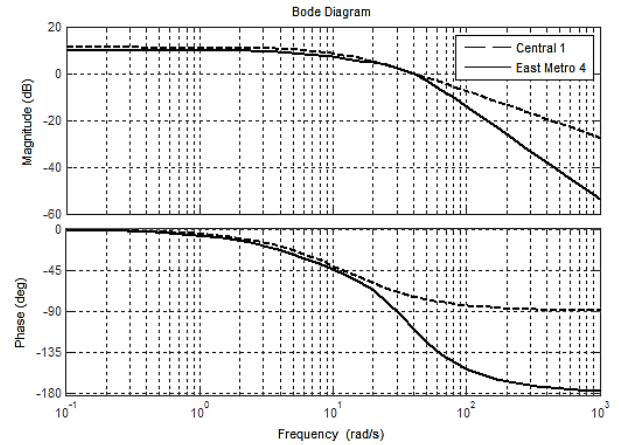
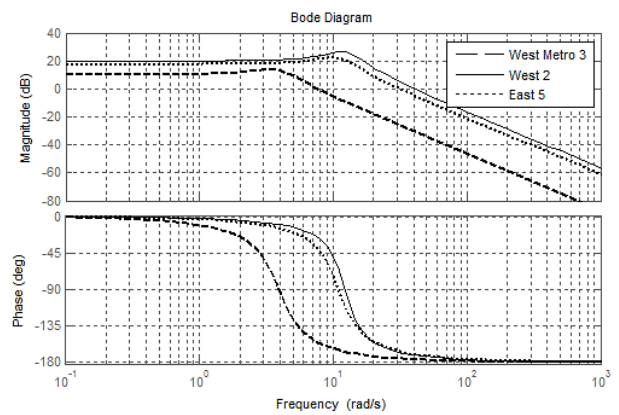

Figure 23: Frequency responses of generators 1, 4

Figure 24: Frequency responses of generators 2, 3 and 5

7. Conclusions

In this paper, the dynamic equations are linearized by considering the high voltage bus of the step-up transformer instead of infinite bus voltage, and all the measurements are local and it does not require overall calculation of system parameters such as equivalent external reactance. The power system stabilizer based on the root locus and frequency response method is used to increase stability and to damp oscillations of 3, 5, and 10 machines systems. The results of these test systems when small disturbances like a 10% step change in V_{ref} or a big disturbance like a 3ϕ fault are applied to the system show the performance of the proposed PSS. However, by using the designed stabilizer, the oscillations will be damped. The results of slip speed response in the three machines system show the superiority of the PSS with lead-lag controller over the PSS with PI controller.

Table 9: PI controller parameters

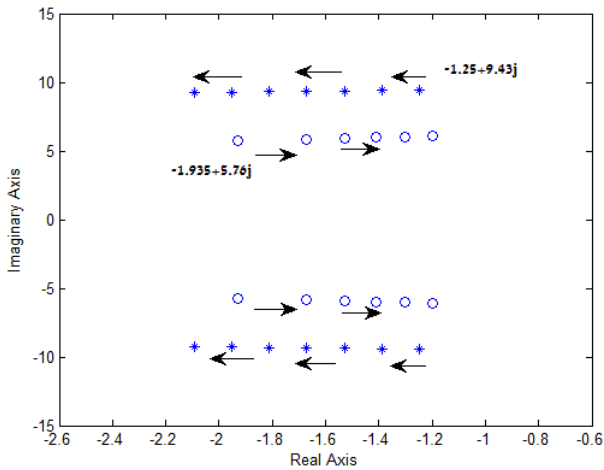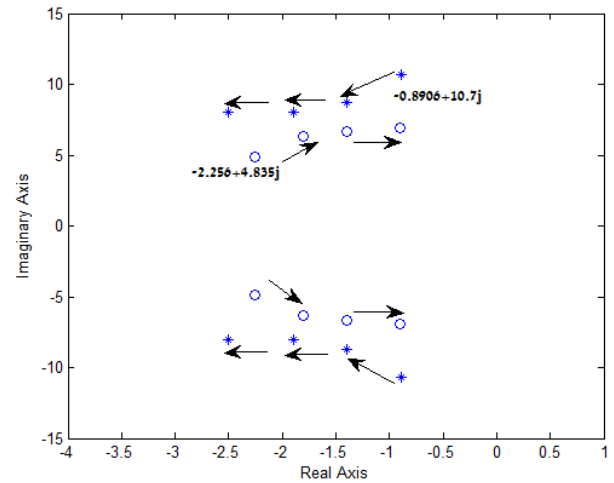| G	K_i	K_p
1	0.005	0.03
2	0.005	0.03
3	0.002	0.07

Figure 25: Variation of eigenvalues with X_t GEN-2, five-generator ten-bus system

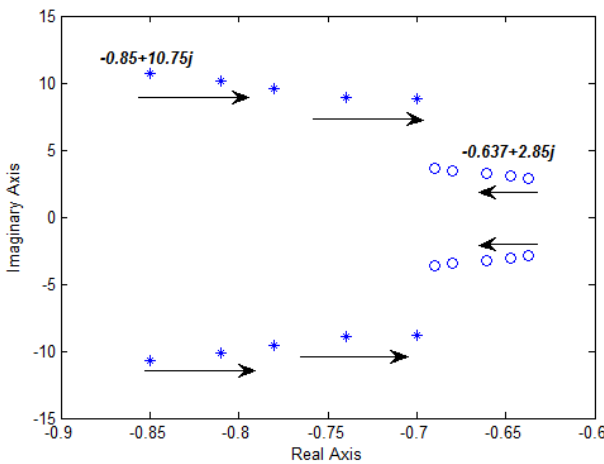Figure 26: Variation of eigenvalues with X_t GEN-3, five-Generator Ten-bus system

Acknowledgments

References

[1] G. Shahgholian, A. Movahedi, Power system stabiliser and flexible alternating current transmission systems controller coordinated design using adaptive velocity update relaxation particle swarm optimisation algorithm in multi-machine power system, IET Generation, Transmission Distribution 10 (2016) 1860–1868.

[2] X. Zhao, L. Shi, L. Chen, Z. Xia, A. Bendre, Modeling and current control strategy for a medium-voltage cascaded multilevel statcom with lcl filter, Journal of Power Technologies 95 (2015) 1–13.

[3] G. Shahgholian, Modelling and simulation of low-head hydro turbine for small signal stability analysis in power system, Journal of Renewable Energy and Environment 3 (2016) 11–20.

[4] M. Farahani, S. Ganjefar, Intelligent power system stabilizer design using adaptive fuzzy sliding mode controller, Neurocomputing 226 (2017) 135–144.

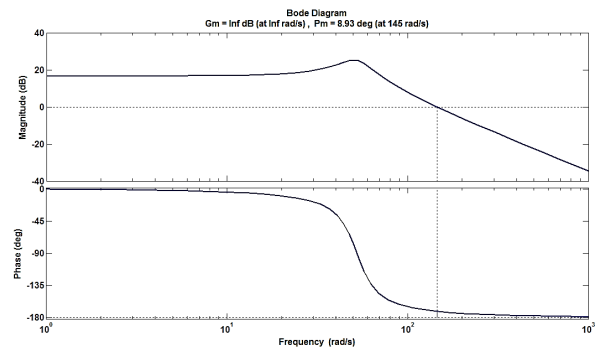Figure 27: Variation of eigenvalues with X_t GEN-5, five-Generator Ten-bus

Figure 28: Frequency responses of generator 5

[5] M. B. A. Jabali, M. H. Kazemi, A new lpv modeling approach using pca-based parameter set mapping to design a pss, Journal of advanced research 8 (2017) 23–32.

[6] G. Shahgholian, M. Ahmadi-Zebarjad, Application of a nonlinear hybrid controller in multi-machine power system based on a power system stabilizer, Journal of Power Technologies 97 (2017) 295–301.

[7] A. Jafari, G. Shahgholian, Analysis and simulation of a sliding mode controller for mechanical part of a doubly-fed induction generator-based wind turbine, IET Generation, Transmission & Distribution 11 (2017) 2677–2688.

[8] G. Shahgholian, Power system stabilizer application for load frequency control in hydro-electric power plant, International Journal of Theoretical and Applied Mathematics 3 (2017) 148–157.

[9] Z. AZIMI, G. SHAHGHOLIAN, Power system transient stability enhancement with tcsc controller using genetic algorithm optimization., International Journal of Natural & Engineering Sciences 10 (2016).

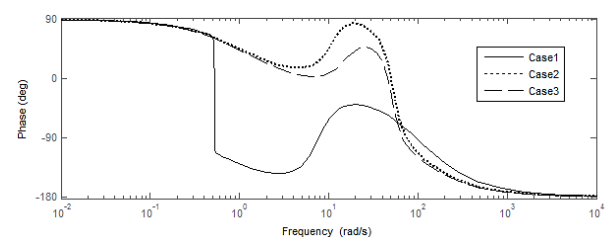[10] H. Quinot, H. Bourles, T. Margotin, Robust coordinated avr+ pss for

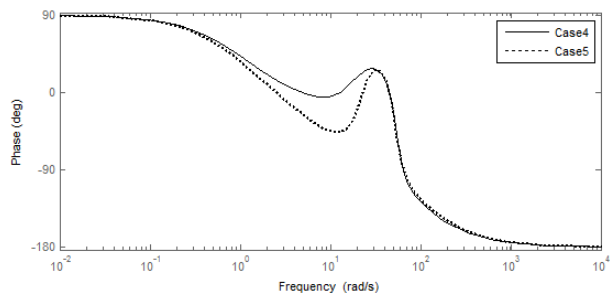Figure 29: Bode plots of GEN-5 for cases 1, 2 and 3
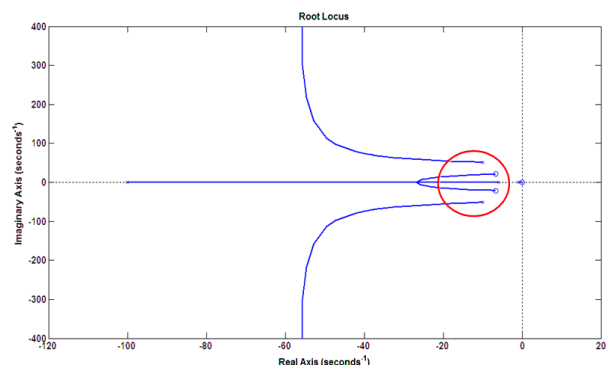
Figure 30: Bode plots of GEN-5 for cases 4 and 5

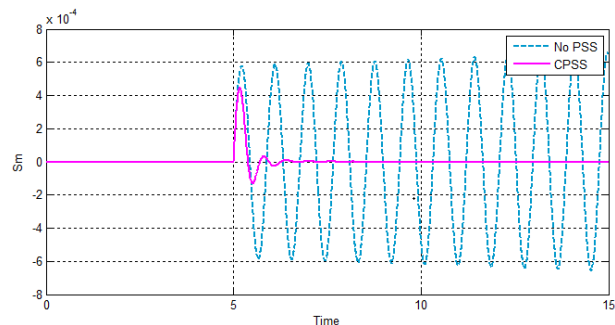
Figure 31: Roots locus of GEN-5 in the fifth state

Figure 33: Slip speed of generator response of GEN-8 to 10% step change in T_m at heavy load condition
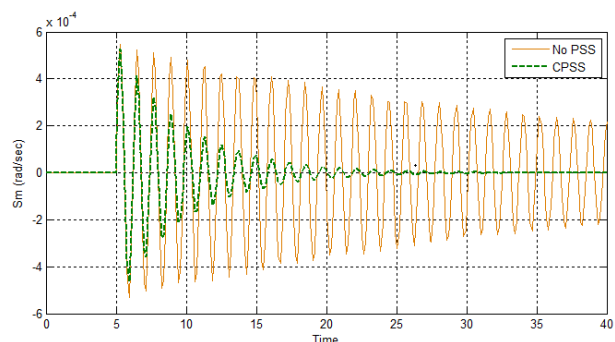

Figure 34: Slip speed response of GEN-6 for a 10% step change in T_m before and after applying the stabilizer

damping large scale power systems, IEEE Transactions on Power Systems 14 (1999) 1446–1451.

[11] A. Shoulaie, M. Bayati-Poudeh, G. Shahgholian, Damping torsional torques in turbine-generator shaft by novel pss based on genetic algorithm and fuzzy logic, Journal of Intelligent Procedures in Electrical Technology 1 (2010) 3–10.

[12] P. M. Anderson, A. A. Fouad, Power system control and stability, John Wiley & Sons, 2008.

[13] G. Shahgholian, J. Faiz, Coordinated control of power system stabilizer and facts devices for dynamic performance enhancement—state of art, in: Intelligent Energy and Power Systems (IEPS), 2016 2nd International Conference on, IEEE, pp. 1–6.

[14] X. Lei, E. N. Lerch, D. Povh, Optimization and coordination of damping controls for improving system dynamic performance, IEEE Transactions on Power Systems 16 (2001) 473–480.

[15] Y. Abdel-Magid, M. Abido, Robust coordinated design of excitation and tcsc-based stabilizers using genetic algorithms, Electric Power Systems Research 69 (2004) 129–141.

[16] N. M. Razali, V. Ramachandaramurthy, R. Mukerjee, Power system stabilizer placement and tuning methods for inter-area oscillation damping, in: Power and Energy Conference, 2006. PECon'06. IEEE International, IEEE, pp. 173–178.

[17] O. Abedinia, N. Amjady, H. Izadfar, H. Shayanfar, Multi-machine power system oscillation damping: Placement and tuning pss via multi-objective hbmo, International Journal of Technical and Physical Problems of Engineering 4 (2012) 12.

[18] G. Shahgholian, Review of power system stabilizer: Application, modeling, analysis and control strategy, International Journal on Technical and Physical Problems of Engineering 5 (2013) 41–52.

[19] A. C. Padoan, B. Kawkabani, A. Schwery, C. Ramirez, C. Nicolet, J.-J. Simond, F. Avellan, Dynamical behavior comparison between variable speed and synchronous machines with pss, IEEE Transactions on Power Systems 25 (2010) 1555–1565.

[20] P. Kundur, M. Klein, G. Rogers, M. S. Zywno, Application of power system stabilizers for enhancement of overall system stability, IEEE Transactions on Power Systems 4 (1989) 614–626.
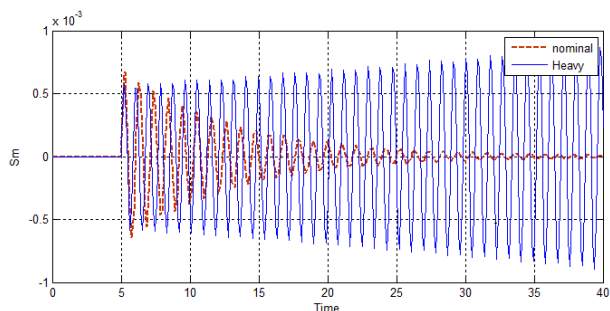
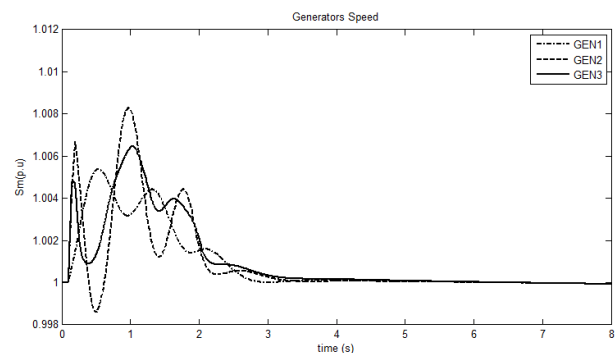Figure 32: Slip speed variations response of GEN-8 to 10% step change in T_m

Figure 35: Slip speed responses of GEN-1 to GEN-3 for a 3ϕ fault with PSS based on the general structure
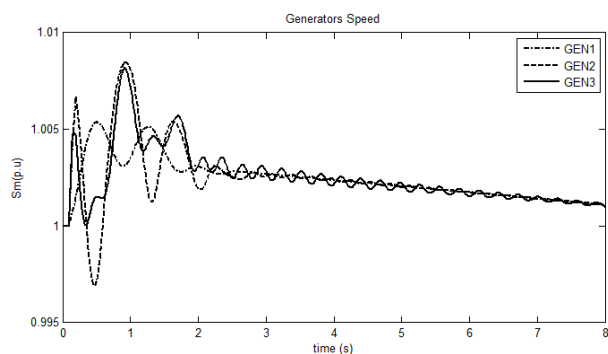
Figure 36: Slip speed responses of GEN-1 to 3 for a 3ϕ fault with PI controller

[21] P. Kundur, N. J. Balu, M. G. Lauby, Power system stability and control, The EPRI Power System Engineering Series ed., McGraw-hill New York, 1994.

[22] P. Sauer, M. Pai, Power system dynamics and stability, Prentice Hall, Upper Saddle River, Nj, 1998.

[23] G. Shahgholian, Development of state space model and control of the statcom for improvement of damping in a single-machine infinite-bus, International Review of Electrical Engineering 4 (2009).

[24] G. Shahgholian, A. Movahedi, J. Faiz, Coordinated design of tcsc and pss controllers using vurpso and genetic algorithms for multi-machine power system stability, International Journal of Control, Automation and Systems 13 (2015) 398–409.

[25] G. Shahgholian, A. Movahedi, Coordinated design of thyristor controlled series capacitor and power system stabilizer controllers using velocity update relaxation particle swarm optimization for two-machine power system stability, Revue Roumaine Des Sciences Techniques 59 (2014) 291–301.

[26] G. Gurrala, I. Sen, Power system stabilizers design for interconnected power systems, IEEE Transactions on Power Systems 25 (2010) 1042–1051.

[27] V. Keumarsi, M. Simab, G. Shahgholian, An integrated approach for optimal placement and tuning of power system stabilizer in multi-machine systems, International Journal of Electrical Power & Energy Systems 63 (2014) 132–139.

[28] G. Shahgholian, M. Mehdavian, M. Azadeh, S. Farazpey, M. Janghorbani, The principle of effect of the transient gain reduction and its effect on tuning power system stabilizer, in: Electrical Engineering/Electronics, Computer, Telecommunications and Information Technology (ECTI-CON), 2016 13th International Conference on, IEEE, pp. 1–6.

[29] M. J. Gibbard, D. J. Vowles, Design of power system stabilizers for a multi-generator power station, in: International Conference on Power System Technology, volume 3, pp. 1167–1171 vol.3.

[30] Y.-N. Yu, Q.-H. Li, Pole-placement power system stabilizers design of an unstable nine-machine system, IEEE transactions on power systems 5 (1990) 353–358.

[31] A. Doi, S. Abe, Coordinated synthesis of power system stabilizers in multimachine power systems, IEEE Transactions on Power Apparatus and Systems (1984) 1473–1479.

[32] K. Padiyar, Power system dynamics: Stability and control, BS publications, Hyderabad, India, 2nd edition, 2002.